Available online at www.sciencedirect.com
ScienceDirect
Ceramics International 35 (2009) 2099–2102
CERAMICS INTERNATIONAL
www.elsevier.com/locate/ceramint

Short communication

γ-Bi_2MoO_6 nanoplates: Surfactant-assisted hydrothermal synthesis and optical properties

Chao Xu, Dingbing Zou, Lihua Wang, Hao Luo, Taokai Ying *

Institute of Physical Chemistry, Zhejiang Normal University, Jinhua 321004, PR China

Received 10 September 2008; received in revised form 28 September 2008; accepted 10 November 2008
Available online 9 December 2008

Abstract

γ-Bismuth molybdate (Bi_2MoO_6) nanoplates were successfully fabricated on a large scale at 180 °C for 12 h by one-step hydrothermal method with the use of surfactant poly(vinyl pyrrolidone) (PVP). X-ray diffraction (XRD), scanning electron microscopy (SEM) and transmission electron microscopy (TEM) were used to characterize the product, and the results indicated that as-prepared Bi_2MoO_6 product had a typical plate-like structure with a thickness range of 100–150 nm. UV–vis spectroscopy was employed to estimate the band gap energy of γ-Bi_2MoO_6 nanoplates, and it exhibited significant absorption from the visible region to near infrared region, in addition to the absorption band in the UV region. The method provides a facile, one-step and low-cost route for the synthesis of nanostructures of multicomponent metal oxides with potential optical applications.

Keywords: B. Electron microscopy; C. Optical properties; Bismuth molybdate; Hydrothermal

1. Introduction

Due to the shape-, size- and dimensionality-dependent properties of nanomaterials and their potential applications, the controlled synthesis of nanostructures has attracted much attention [1]. A considerable number of these materials with various morphologies have been prepared and investigated hitherto in many areas [2,3].

γ-Bi_2MoO_6, as an Aurivillius-phase perovskite, belongs to the bismuth oxide family with a structure consisting of perovskite layers between bismuth oxide layers, with a general formula $[Bi_2O_2][A_{n-1}B_nO_{3n+1}]$ [4,5]. It has been found that γ-Bi_2MoO_6 can be used as ionic conductor [6,7], catalyst for CO conversion [8,9], catalyst for the selective oxidation and ammoxidation of lower olefins [5,10,11], photocatalyst for water splitting under visible-light irradiation [12], and, most importantly, as visible-light responsive photocatalyst for the degradation of organic pollutants [13–15]. Various methods, such as solid-state reaction [10,16], spray drying [11,17], reflux method [12], microwave- and ultrasonic-assisted synthesis [13,14,18], molten method [15], and conventional hydrothermal synthesis [7,19] have been used to prepare γ-Bi_2MoO_6. Recently, the soft chemical method has been demonstrated to be convenient and economical-friendly in synthesizing nanosized γ-Bi_2MoO_6 [13–15,19]. However, they were usually conducted at specific pH values, and needed a further calcination procedure, which involved the complex, high-energy and environmentally unfriendly conditions. Hence, to synthesize γ-Bi_2MoO_6 nanomaterials by a facile and one-step route still remains a significant challenge.

In this communication, we present a facile, one-step hydrothermal method for fabricating γ-Bi_2MoO_6 nanoplates at a relatively low temperature of 180 °C with the use of surfactant PVP. To our best knowledge, PVP-assisted hydrothermal route has not been employed to prepare γ-Bi_2MoO_6 species. In addition, the preliminary results of the optical properties of γ-Bi_2MoO_6 nanoplates are also reported.

2. Experimental

All chemicals are of analytical grade used without further treatments. In a typical procedure, 0.242 g (1 mmol) of $Na_2MoO_4{\cdot}2H_2O$ and 0.971 g (2 mmol) of $Bi(NO_3)_3{\cdot}5H_2O$ were, respectively dissolved in 40 mL of distilled water under

* Corresponding author. Tel.: +86 579 82282780; fax: +86 579 82282269.
E-mail address: sky50@zjnu.cn (T. Ying).

0272-8842/$34.00
doi:10.1016/j.ceramint.2008.11.016

constant stirring. 0.15 g of PVP K30 was added to the Na_2MoO_4 aqueous solution to form a homogeneous mixture. After that, the mixture was subsequently dropped to the $Bi(NO_3)_3$ aqueous solution slowly, and then transferred into a 100 mL Teflon-lined stainless steel autoclave. The autoclave was sealed and maintained at 180 °C for 12 h, followed by cooling to room temperature naturally. The resulting product was filtered off, washed with distilled water and absolute ethanol in sequence, and then dried in a vacuum at 60 °C for 6 h. A control experiment was also carried out in the absence of PVP while keeping other experimental conditions unchanged.

The crystalline structure of the product was analyzed by an X-ray diffractometer (XRD, Philps-PW3040/60) with Cu Kα radiation (λ = 0.15418 nm). The morphologies of as-prepared products were characterized by scanning electron microscopy (SEM, HITACHI S-4800) operated at an acceleration voltage of 5.0 kV. Transmission electron microscopy (TEM) observations were carried out using a JEOL-2010 instrument at an accelerating voltage of 200 kV. UV–vis diffuse reflectance spectra of as-prepared products were obtained on an UV–vis spectrophotometer (Evolution 500) using $BaSO_4$ as reference.

3. Results and discussion

XRD patterns of γ-Bi_2MoO_6 products synthesized by the hydrothermal method without and with the addition of surfactant PVP are, respectively shown in Fig. 1(a) and (b). All of the diffraction peaks in the two XRD patterns can be clearly indexed as an orthorhombic phase of Bi_2MoO_6 (Aurivillius structure) and match very well with the reported data (JCPDS card No. 84-0787). No extra peaks arising from other phases can be detected, indicating pure γ-Bi_2MoO_6 can be obtained by the present hydrothermal process. In addition, it is noteworthy that some diffraction peaks in Fig. 1(b), especially (1 3 1), become stronger and sharper compared with that in Fig. 1(a). This comparison indicates that better crystallization of γ-Bi_2MoO_6 can be realized in the PVP-assisted hydrothermal process.

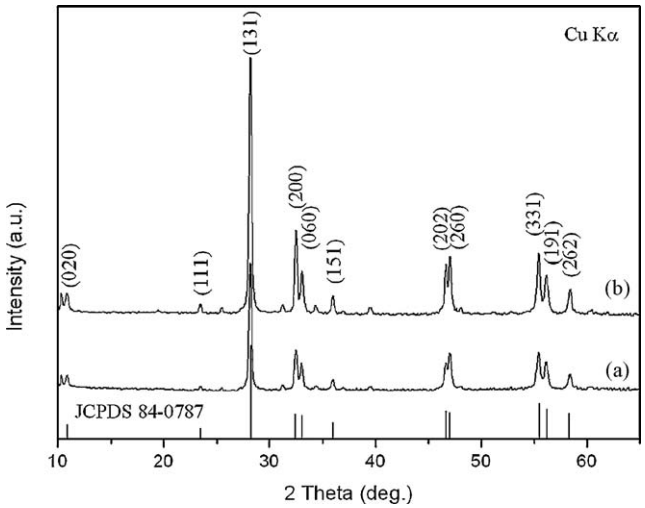

Fig. 1. X-ray diffraction patterns of as-prepared Bi_2MoO_6 by the hydrothermal method (a) without and (b) with the addition of surfactant PVP.

The morphological images of γ-Bi_2MoO_6 product obtained in the presence of PVP are shown in Fig. 2. Fig. 2(a) is a low-magnification SEM image of this product, from which a typical flowery architecture consisting of smooth plates is clearly observed. No other morphologies could be detected, indicating a high yield of plate-like structures. The high-magnification SEM image shown in Fig. 2(b) demonstrates that these plates have a relatively uniform thickness range of 100–150 nm, and are irreversibly connected at their junctions to form the self-assembly structure. The corresponding TEM images of the product are shown in Fig. 2(c)–(e). Due to the action of

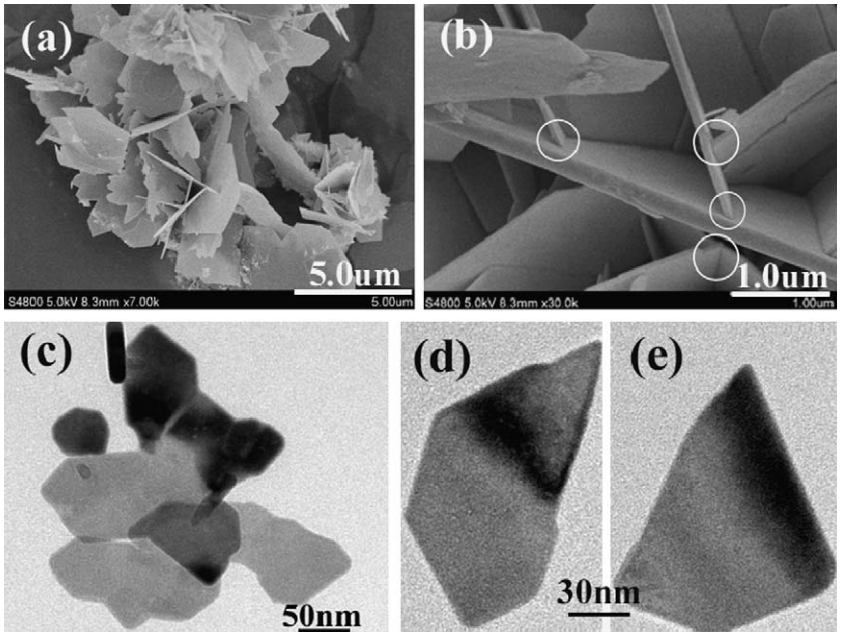

Fig. 2. SEM (a and b) and TEM images (c–e) of Bi_2MoO_6 nanoplates synthesized by the hydrothermal method assisted by surfactant PVP.

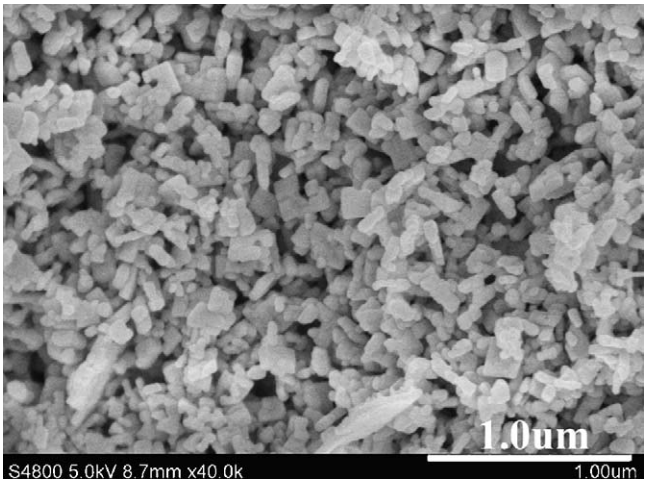

Fig. 3. SEM image of Bi_2MoO_6 nanoparticles synthesized by the hydrothermal method in the absence of surfactant PVP.

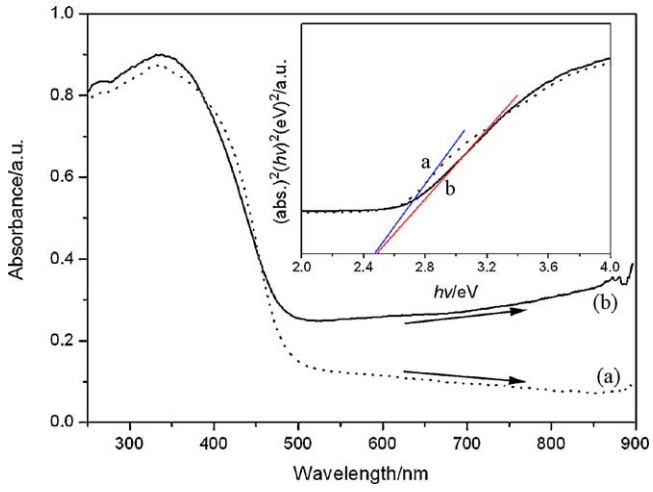

Fig. 4. UV–vis diffuse reflectance spectrum of Bi_2MoO_6 products synthesized by the hydrothermal method (a) without and (b) with the addition of PVP.

sonication during the preparation of specimens for TEM observation, the total morphology of the self-assembly structure is destroyed, and only some smaller nanoplates with various shapes can be observed.

The growth mechanism for the formation of γ-Bi_2MoO_6 nanoplates is still unclear in the process of the synthesis, but we believe that PVP plays an important role in the formation of γ-Bi_2MoO_6 nanoplates. In the absence of PVP, γ-Bi_2MoO_6 with a different morphology can be obtained as shown in Fig. 3. It can be seen that this product consists of nanoparticles with a size of 100–200 nm, and few nanoplates are indeed observed.

UV–vis diffuse reflectance spectra of γ-Bi_2MoO_6 products synthesized by the hydrothermal method without and with the addition of PVP are, respectively shown in Fig. 4(a) and (b). It can be seen that they both have the steep absorption edges located at ∼500 nm for nanoparticles and ∼496 nm for nanoplates, indicating that the absorption relevant to the band gap is due to the intrinsic transition of the nanomaterials rather than a transition from impurity levels [20]. According to the equation $\alpha h\nu = A(h\nu - E_g)^{1/2}$, where α, h, ν, E_g, and A are absorption coefficient, Planck constant, light frequency, band gap, and a constant, respectively, the energy can be estimated to be ∼2.48 eV for nanoparticles and ∼2.50 eV for nanoplates (the inset shows the plot of $(\alpha h\nu)^2 \sim h\nu$ based on the direct transition). Meanwhile, the latter exhibits a significant absorption with a gradually enhanced absorbance in the region from 500 nm to in excess of 900 nm compared with that of the former, in addition to the absorption band at wavelength below 500 nm. As it is known, UV light accounts for merely 5% of the solar spectrum, and thus the extended activity of photocatalyst in the visible region generally improves the efficiency of photocatalyst [21]. Thus, the as-prepared γ-Bi_2MoO_6 nanoplates have a potential photocatalytic activity with higher efficiency over those γ-Bi_2MoO_6 materials [12–14]. The unusual optical phenomena may be associated with the plate-like shape and their self-assembled structures.

4. Conclusions

γ-Bi_2MoO_6 nanostructures with typical plate-like morphology have been synthesized by a facile PVP-assisted hydrothermal method at 180 °C for 12 h, and the as-prepared γ-Bi_2MoO_6 nanoplates exhibit unusual UV–vis characteristics. The present study will not only open up great opportunities for the synthesis of γ-Bi_2MoO_6 species with potential optical applications, but might also be extended to the controlled syntheses of other multicomponent metal oxides.

References

[1] X.F. Wu, H. Bai, C. Li, G.W. Lu, G.Q. Shi, Controlled one-step fabrication of highly oriented ZnO nanoneedle/nanorods arrays at near room temperature, Chem. Commun. (2006) 1655–1657.
[2] X. Peng, Green chemical approaches toward high-quality semiconductor nanocrystals, Chem. Eur. J. 8 (2002) 335–339.
[3] Z.Q. Li, Y. Ding, Y.J. Xiong, Q. Yang, Y. Xie, Room-temperature surface-erosion route to ZnO nanorod arrays and urchin-like assemblies, Chem. Eur. J. 10 (2004) 5823–5828.
[4] R. Rangel, P. Bartolo-Perez, A. Gomez-Cortes, G. Diaz, D.H. Galvan, Study of microstructure and catalytic activity of γ-Bi_2MoO_6 and Bi_2WO_6 compounds, Surf. Rev. Lett. 9 (2002) 1779–1783.
[5] D.J. Buttrey, T. Vogt, B.D. White, High-temperature incommensurate-to-commensurate phase transition in the Bi_2MoO_6 catalyst, J. Solid State Chem. 155 (2000) 206–215.
[6] R. Murugan, Investigation on ionic conductivity and raman spectra of γ-Bi_2MoO_6, Phys. B 352 (2004) 227–232.
[7] Y.H. Shi, S.H. Feng, C.S. Cao, Hydrothermal synthesis and characterization of Bi_2MoO_6 and Bi_2WO_6, Mater. Lett. 44 (2000) 215–218.
[8] R. Rangel, P. Bartolo-Perez, A. Gomez-Cortes, G. Diaz, S. Fuentes, D.H. Galvan, Comparison between γ-Bi_2MoO_6 and Bi_2WO_6 catalysts in the CO oxidation, J. Mater. Synth. Process. 9 (2001) 207–212.
[9] D.H. Galvan, S. Fuentes, M. Avalos-borja, L. Cota-Araiza, Structure and catalytic activity characterization of bismuth molybdate catalysts, Catal. Lett. 18 (1993) 273–281.
[10] S. Williams, M. Puri, A.J. Jacobson, C.A. Mims, Propene oxidation on substituted 2:1 bismuth molybdates and vanadates, Catal. Today 37 (1997) 43–49.
[11] M.T. Le, W.J.M. Van Well, I. Van Driessche, S. Hoste, Influence of organic species on surface area of bismuth molybdate catalysts in complexation and spray drying methods, Appl. Catal. A 267 (2004) 227–234.

[12] Y. Shimodaira, H. Kato, H. Kobayashi, A. Kudo, Photophysical properties and photocatalytic activities of bismuth molybdates under visible light irradiation, J. Phys. Chem. B 110 (2006) 17790–17797.
[13] J.H. Bi, L. Wu, J. Li, Z.H. Li, X.X. Wang, X.Z. Fu, Simple solvothermal routes to synthesize nanocrystalline Bi_2MoO_6 photocatalysts with different morphologies, Acta Mater. 55 (2007) 4699–4705.
[14] L. Zhou, W.Z. Wang, L.S. Zhang, Ultrasonic-assisted synthesis of visible-light-induced Bi_2MO_6 (M = W, Mo) photocatalysts, J. Mol. Catal. A 268 (2007) 195–200.
[15] L.J. Xie, J.F. Ma, G.J. Xu, Preparation of a novel Bi_2MoO_6 flake-like nanophotocatalyst by molten salt method and evaluation for photocatalytic decomposition of rhodamine B, Mater. Chem. Phys. 110 (2008) 197–200.
[16] A. Kudo, S. Hijii, H_2 or O_2 evolution from aqueous solutions on layered oxide photocatalysts consisting of Bi^{3+} with $6s^2$ configuration and d^0 transition metal ions, Chem. Lett. 10 (1999) 1103–1104.
[17] M.T. Le, W.J.M. Van Well, P. Stoltze, I. Van Driessche, S. Hoste, Synergy effects between bismuth molybdate catalyst phases (Bi/Mo from 0.57 to 2) for the selective oxidation of propylene to arcrolein, Appl. Catal. A 282 (2005) 189–194.
[18] H.D. Xie, D.Z. Shen, X.Q. Wang, G.Q. Shen, Microwave hydrothermal synthesis and visible-light photocatalytic activity of γ-Bi_2MoO_6 nanoplates, Mater. Chem. Phys. 110 (2008) 332–336.
[19] A.M. Beale, G. Sankar, In situ study of the formation of crystalline bismuth molybdate materials under hydrothermal conditions, Chem. Mater. 15 (2003) 146–153.
[20] Y.Y. Li, J.P. Liu, X.T. Huang, G.Y. Li, Hydrothermal synthesis of Bi_2WO_6 uniform hierarchical microspheres, Cryst. Growth Des. 7 (2007) 1350–1355.
[21] X.X. Wang, S. Meng, X.L. Zhang, H.T. Wang, W. Zhong, Q.G. Du, Multi-type carbon doping of TiO_2 photocatalyst, Chem. Phys. Lett. 444 (2007) 292–296.